

Research Article

Process Integration of Hydrogen Production Using Steam Gasification and Water-Gas Shift Reactions: A Case of Response Surface Method and Machine Learning Techniques

Anthony Ikechukwu Okoji ¹, Abiola Ezekiel Taiwo ², John Busayo Adeoye ³, Paul Musonge ², David Olamide Makinde,⁴ and Comfort Nneka Okoji⁵

¹Department of Chemical Engineering, Covenant University, Ota, Ogun State, Nigeria

²Faculty of Engineering, Mangosuthu University of Technology, Durban 4026, South Africa

³Department of Chemical and Energy Engineering, Faculty of Engineering and Science, Curtin University Malaysia, CDT 250, 98009 Miri, Sarawak, Malaysia

⁴Department of Chemical Engineering, Landmark University, Omu-Aran, Kwara State, Nigeria

⁵Department of Biology and Forensic, Admiralty University, Ibusa, Delta State, Nigeria

Correspondence should be addressed to Abiola Ezekiel Taiwo; taiwo.abiola@mut.ac.za

Received 11 November 2023; Revised 28 December 2023; Accepted 15 May 2024; Published 29 May 2024

Academic Editor: Geng Chen

Copyright © 2024 Anthony Ikechukwu Okoji et al. This is an open access article distributed under the Creative Commons Attribution License, which permits unrestricted use, distribution, and reproduction in any medium, provided the original work is properly cited.

An equilibrium-based steady-state simulator model that predicts and optimizes hydrogen production from steam gasification of biomass is developed using ASPEN Plus software and artificial intelligence techniques. Corn cob's chemical composition was characterized to ensure the biomass used as a gasifier and with potential for production of hydrogen. Artificial intelligence is used to examine the effects of the significant input variables on response variables, such as hydrogen mole fraction and hydrogen energy content. Optimizing the steam-gasification process using response surface methodology (RSM) considering a variety of biomass-steam ratios was carried out to achieve the best results. Hydrogen yield and the impact of main operating parameters were considered. A maximum hydrogen concentration is found in the gasifier and water-gas shift (WGS) reactor at the highest steam-to-biomass (S/B) ratio and the lowest WGS reaction temperature, while the gasification temperature has an optimum value. ANFIS was used to predict hydrogen of mole fraction, 0.5045 with the input parameters of S/B ratio of 2.449 and reactor pressure and temperature of 1 bar and 848°C, respectively. With the steam-gasification model operating at temperature (850°C), pressure (1 bar), and S/B ratio of 2.0, an ASPEN simulator achieved a maximum of 0.5862 mole fraction of hydrogen, while RSM gave an increase of 19.0% optimum hydrogen produced over the ANFIS prediction with the input parameters of S/B ratio of 1.053 and reactor pressure and temperature of 1 bar and 850°C, respectively. Varying the gasifier temperature and S/B ratio have, on the other hand, a crucial effect on the gasification process with artificial intelligence as a unique tool for process evaluation, prediction, and optimization to increase a significant impact on the products especially hydrogen.

1. Introduction

Human development has been challenged by the depletion of energy resources, impacts on the environment, and insecurities around national energy security due to increased energy demand and consumption [1]. Biomass is one of the renewable energy sources that does not involve the emis-

sion of greenhouse gases, unlike fossil fuels with many pollutants [2, 3]. Renewable energy is an alternative energy generation that has gained traction for some time, as its sources have a greater presence in the modern world energy market. Human civilization and technological advancement are leading to an increase in global energy demand. The world's energy security has been threatened by rapidly

diminishing fossil fuel reserves [4]. Thus, in response to these problems, continuous efforts have been made to explore clean, renewable alternatives for sustainable development to transition the world from overdependence on fossil fuels gradually [5]. However, alternative energy sources such as hydrogen production, bioethanol, and biogas [6] are proving to be safe and effective means to an extent, addressing the issues mentioned earlier. Global energy consumption was 18.1% fueled by renewable energy sources in 2017, with biomass contributing 12.1% [7], which establishes it as a potentially viable and more advantageous energy source when compared to fossil fuels. It is widely acknowledged that hydrogen serves as an attractive energy source to replace conventional fossil fuels from an economic standpoint as well as from an environmental perspective. Biomass is among the most readily available and abundant renewable energy resources because of its carbon neutrality [8]. In a recent study by Park et al. [9], the authors propose a corn biomass to syngas chemical looping system for a range of downstream applications, with focus on liquid fuel production. The study reported a variable syngas quality with an H_2/CO ratio of approximately 2, and a syngas purity greater than 70% was achieved. A comprehensive comparative study using multicriteria decision analysis was conducted on the gasification of waste polymeric foam at multiobjective optimum conditions using response surface methodology [10]. Another study by Hasanzadeh et al. [11] models and optimizes the performance of the gasification of a rice husk and low-density polyethylene waste composite, and the authors reported an energy efficiency of 77.6%. A high degree of accuracy can be achieved using the ASPEN Plus software model for different gasifiers (air gasification or steam gasification) this simulator could predict high syngas compositions from different biomasses. In a study that assessed the potential for lignocellulosic biomass to be converted to butanol using chemical looping gasification, Li et al. [12] established an ASPEN Plus model, which shows an efficiency of 45.33%. A partial gasification model using ASPEN Plus was developed by Zhang et al. [13]. At the same time, different thermodynamic analyses were performed, such as exergy, energy, and economic analyses. The gasification process that was reported with key input parameters yielded cold gas and energy efficiency of 46.08 and 67.08%, respectively, and a net heat efficiency of 44.25% at a carbon conversion ratio of 0.7. In another study that used the ASPEN Plus model for biomass gasifier, Pala et al. [14] demonstrated that a shift reaction could be used to tune the syngas composition successively and achieved a molar ratio of about 2.15 for H_2 and CO. A 35 kVA downdraft biomass gasifier was modeled using ASPEN Plus simulated by Keche et al. [15], and babul wood was found to produce more H_2 in the syngas than other biomass used as feedstocks. In a model that predicts the result with less error than experimental results in temperatures between 700 and 900°C, Pauls et al. [16] used air and steam as gasifying agents.

The response surface methodology (RSM) is widely used for optimizing new and existing systems [17]. The one factor at a design approach is not cost and time effective. Response surface methodology (RSM) is one of the most applicable designs of experimental methods [18]. RSM helps to present a regression model to predict the response variable based on the considered input parameters [19, 20]. In addition to

RSM, genetic algorithms (GA) can be used to optimize any process or system. Nevertheless, RSM offers adequate accuracy for optimizing processes or systems (almost identical to GA). According to a previous study [21], RSM provides better optimization accuracy than GA. Furthermore, GA relies on a heuristic optimization strategy, which does not guarantee optimal solutions.

The optimization of biomass, coal, and waste torrefaction process variables made use of artificial neural networks and RSM by Ozonoh et al. [22]. In comparison with raw fuel, the torrefied product showed 10% higher heating values. Based on RSM, Inayat et al. [23] optimized the catalytic cogasification of palm waste and found that the gasification temperature and the catalytic loading and blending ratio are the most influential. Optimal conditions resulted in 19.96% CH_4 and 38.81% syngas. In a study of hydrothermal gasification (HTG), Fozer et al. [24] used RSM for optimizing microalgae biomass production and sequential biogas generation. In optimum light levels, fermentation of microalgae biomass produces H_2 -rich gas without requiring any catalyst, suggesting improvement at the farm stage in downstream processing. As part of the optimization of a design mix of palm oil and diesel fuel introduced into diesel engines, Uslu [25] utilized RSMs and artificial neural networks (ANNs).

Fuzzy inference systems are generated using ANFIS-based methods, such as grid partition, subclustering, and fuzzy c-means. Multiple and individual response variables have been used in this study to optimize the equilibrium gasifier model. To compare BP-ANN and ANFIS models with the ASPEN Plus process model, extensive simulation studies are conducted to determine the best predictive model. Furthermore, synchronized effects among input and response variables determined optimal operating conditions for steam gasification.

Any gasification process requires optimization to achieve high-quality syngas. Thus, no detailed predictive models have been developed using back propagation neural networks (BP-ANN) and ANFIS, statistical analysis, and syngas production optimization for a developed steam-gasification process. This present study combines back propagation artificial neural network BP-ANN and adaptive neuro fuzzy inference system (ANFIS) to develop a prediction model for biomass gasification based on ASPEN Plus simulation. The use of artificial intelligence integrated with process simulations will help provide relevant industrial conditions as a result of energy concerns. The process will provide the opportunity to understand and design an optimal hydrogen production scale-up.

2. Materials and Methods

This study used plant raw materials that are annually renewable in Nigeria and concentrated in growing or processing sites. Corn cob, rice husk, and coconut shell were collected during grain crop harvesting. Plant material was air-dried and crushed to particle sizes (<1 mm) on a disintegrator. Furthermore, some parameters, including the identified biomass's fixed carbon and volatile matter, were determined using the ASTM standard. Using standard methods

established in the literature, the samples' percentages of moisture and ash were determined [26].

An elemental analysis (proximate and ultimate analysis) was performed on biomass materials such as corn cob and was found to have a moderately higher calorific value, as shown in Table 1. This represents the input parameters in ASPEN Plus for the gasification reaction process for syngas, especially hydrogen. Detailed and comprehensive studies on characterization of corn cob for application in a gasification process for energy production have been reported in literature [27]. The results of the authors are comparable to the current study corn cob analysis.

3. Model Description

3.1. ASPEN Plus Model, Equation, and Assumptions. A Gibbs free energy minimization equilibrium model was used in this study as represented in Eq. (1). This equilibrium model is computationally economical yet supplies valuable information about gasification at high temperatures [28]. Based on Rupesh et al. [29], the Gibbs free energy can be expressed as the sum of moles (n) and chemical potential (μ) of reacting species (i).

$$G_T = \sum_{i=1}^N n_i \mu_i. \quad (1)$$

For the minimization of the Gibbs free energy, it is possible to apply the Lagrange multiplier method, which gives the following equation.

$$\frac{\partial L}{\partial n_i} = \Delta G_{f,i}^0 + n_i RT \ln \left(\frac{n_i}{n_{\text{total}}} \right) + \sum_{j=1}^k a_{ij} \lambda_j. \quad (2)$$

Thus, L is the Lagrange function, while the Lagrange multiplier is λ_j .

Gibbs free energy and Lagrange multipliers presented in Equations (1) and (2) have been applied in previous studies [30]. The biomass gasification process model flowsheet diagram for the corn cob is displayed in Figure 1. As a result of adopting the Peng-Robinson equation of state [31, 32] in the property method section, excellent precision could be obtained when simulating biomass steam gasification processes. Biomass was classified as a nonconventional input, and its proximate and ultimate analyses were entered in the stream named "Biomass" under "component attributes." Moreover, steam is supplied at 150°C and 1 bar as a gasifying agent. A Gibbs reactor (RGIBBS) was operated with varying steam mass flow rates and variable biomass inputs to alter the steam-to-biomass ratio (S/B) and temperature in the gasification process (T). The blocks (reactors) used for the ASPEN Plus gasification's simulations for the corn cob are shown in Table 2.

This model is simplified by making the following assumptions: (i) Simulating atmospheric conditions and steady-state conditions is carried out; (ii) initially, devolatilization occurs instantaneously; (iii) a negligible amount of

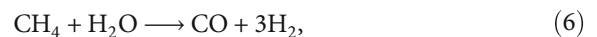
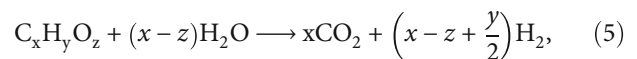
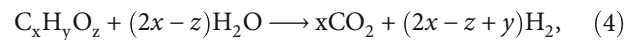
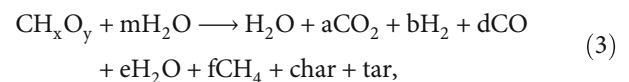
TABLE 1: Corn cob elemental analysis.

| Proximate analysis, dry basis (%) | | | | | Ultimate analysis, dry basis (%) | | | | |
|-----------------------------------|-----|------|------|-------|----------------------------------|-----|-----|------|---|
| M | A | VM | FC | HHV | C | H | N | O | S |
| 9.8 | 8.5 | 69.2 | 12.5 | 17.04 | 47.2 | 6.4 | 0.4 | 46.0 | 0 |

M: moisture; A: ash; VM: volatile matter; FC: fixed carbon; HHV: high heating value (MJ/kg).

heat is lost; (iv) ash is considered an inert substance. In addition, the experimental statistical data range from the ASPEN Plus process model is shown in Table 3.

The biomass biodegradation reaction, steam reforming with methanization, and gas-water shift reactions are presented in different conditions. The process for this reaction is presented in [33]



3.2. Models Based on BP and ANN. The BP-ANN is one of the most widely used ANNs [34, 35]. This is a multilayer feedforward neural network that uses Rumelhart and McClelland's error backpropagation algorithm, first proposed in the 1980s [36]. The input, hidden, and output layers of BP-ANN can be divided into three sublayers, with the hidden layer including one or more sublayers as shown in Figure 2. Thus, an ANN with a BP sigmoid function is widely used to activate a neuron as shown in Eq. (8): Equations (8)–(10) have been applied in our previous study [37].

$$f(s) = \frac{1}{1 + e^{-s}}, \quad (8)$$

where s denotes the input variable's value.

Neurons in the hidden layer and outer layer of a BP-ANN can be expressed as outputs:

$$t_i = f(\text{net}_j) = f\left(\sum_i \omega_{ji} s_i - \theta_j\right), \quad (9)$$

$$u_l = f(\text{net}_l) = f\left(\sum_i \rho_{jl} s_i - \theta_j\right). \quad (10)$$

where s_i , t_j , and u_l represent inputs and outputs, $f(\text{net})$ represents the transfer function, ω and ρ are weight vectors of input layer and hiding layer, and θ is the threshold value of the neuron.

Net = newff (X, Y, 'trainfun, 'trainlm) in MATLAB creates the BP model: X is the maximum and minimum value

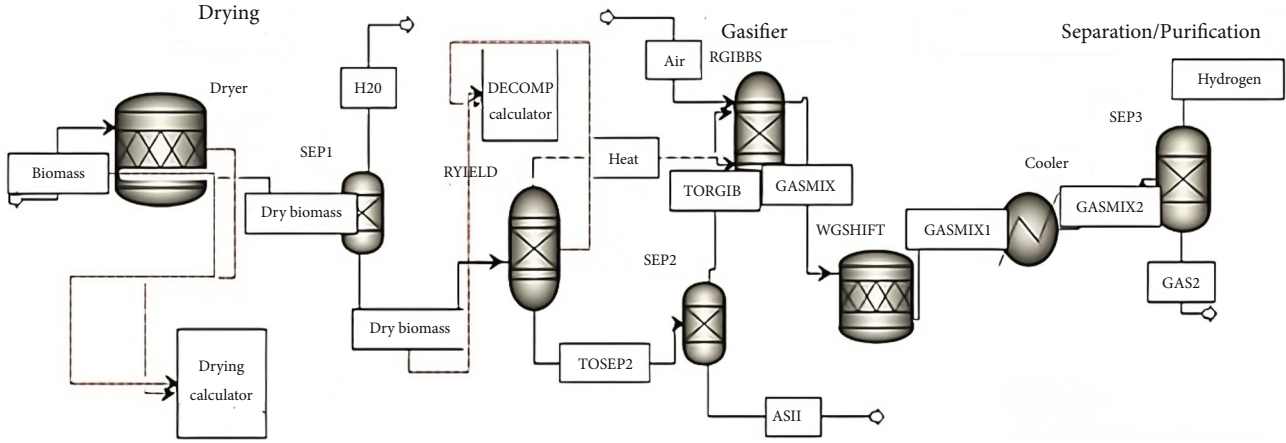


FIGURE 1: ASPEN Plus process flow diagram for gasification.

TABLE 2: ASPEN Plus blocks and model representation for biomass steam gasification.

| Block | Model | Function |
|-------------------|--------|--|
| DRYING | RYIELD | Biomass is either dried based on proximate analysis of water content or divided into conventional components and ash |
| BIOMASS-DECOMPOSE | RSTOIC | For simulation of biomass gasification and combustion, decompose biomass into CO, CO ₂ , H ₂ , CH ₄ , N ₂ , and ash to easily handle solid reactions |
| SEP | SEP | Rotation and gravitational forces are used to separate gas and solid impurities |
| RGIBBS | | Gasification reactions occur when the Gibbs free energy minimization is applied to all possible reactions |
| SSPLIT | | A yield reactor creates char, RSTOIC produces H ₂ S after formation, and dry syngas is obtained by separating H ₂ O from syngas |

TABLE 3: Experimental data range from the ASPEN Plus process model.

| Parameters | Unit | Minimum | Mean | Maximum |
|---------------------|------|---------|----------|---------|
| Input | | | | |
| Steam | kg/h | 5500 | 34952.88 | 60000 |
| Reactor pressure | Bar | 0.1 | 0.15 | 1.0 |
| Reactor temperature | °C | 360 | 627.6 | 850 |
| Biomass | kg/h | 10000 | 20000 | 30000 |
| Output | | | | |
| Mole fraction | | | | |
| H ₂ | | 0.17 | 0.387 | 0.5862 |
| CO ₂ | | 0.072 | 0.123 | 0.145 |
| CO | | 0.01 | 0.099 | 0.332 |
| CH ₄ | | 0.00 | 0.00 | 0.022 |

of the input quantity, Y is the number of hidden layer nodes, 'trainfun' is the transfer function (tansig function was used in this case), and 'trainlm' is the training function.

In this study, the steam flow (kg/h), reactor pressure (bar), reactor temperature (°C), and biomass flow (kg/h) are considered input data, and the amount of H₂ (mole fraction) and, in the network training, hydrogen energy content (MJ/kg) was considered an output of the process. Training, validation, and test sets of data points for the ANN are divided into three categories, whose percentages are adjustable [36].

3.3. *ANFIS Model Building.* A model was developed using four (4) parameters which are independent variables, the steam flow (kg/h), reactor pressure (bar), reactor temperature (°C), and biomass flow (kg/h) as input while the output set contains data of the amounts of H₂ (mole fraction) and energy content of the hydrogen produced (MJ/kg). These variables are listed in Table 3 along with their statistical characteristics. All subgroups have quite large ranges of data for each variable.

MATLAB functions linked to ANFIS are used to build model programs; the ANFIS model structure is shown in Figure 3. In general, a subject expert describes the fuzzy rules. The algorithm rather than an expert creates the rules when ANFIS is used. Two strategies were investigated in this study for generating a fuzzy inference system (FIS) structure from ANFIS data [38].

For this study, a first-order Sugeno-type model was built using four input variables and IF-THEN fuzzy logic. Fuzzy rules, assuming two inputs (x, y) and one output (f), are as follows according to equations (11) and (12) of the fuzzy inference method (FIS):

$$\text{Rule 1} \longrightarrow \text{if } x \text{ is } A_1 \text{ and } y \text{ is } B_1, \text{ then } f_1 = p_1x + q_1y + r_1, \quad (11)$$

$$\text{Rule 2} \longrightarrow \text{if } x \text{ is } A_2 \text{ and } y \text{ is } B_2, \text{ then } f_2 = p_2x + q_2y + r_2. \quad (12)$$

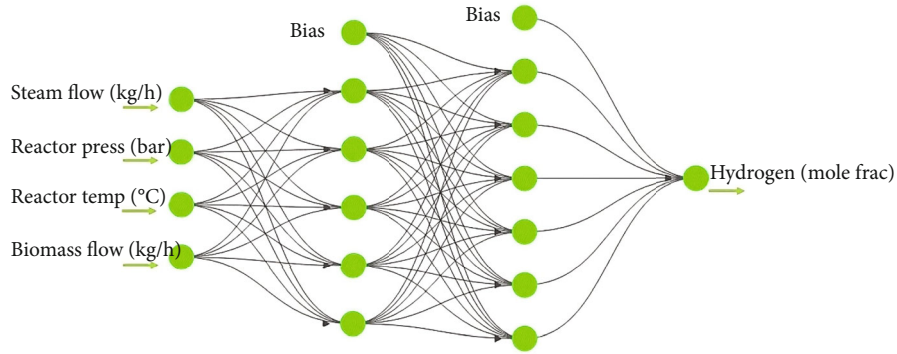


FIGURE 2: Typical BP-ANN network architecture.

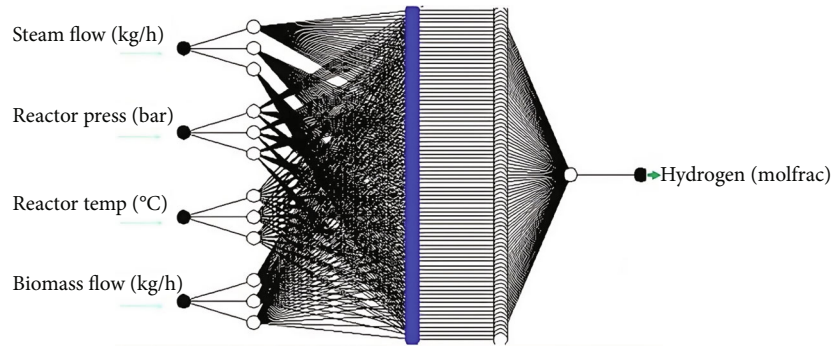


FIGURE 3: ANFIS network model architecture.

TABLE 4: Statistical models for evaluation.

| Equations |
|---|
| $R^2 = 1 - \frac{\sum_{i=1}^n (Y_{i,pre} - Y_{i,exp})^2}{\sum_{i=1}^n (Y_{i,exp} - Y_m)^2}$ |
| $MAE = \frac{1}{n} \sum_{i=1}^n Y_{i,exp} - Y_{i,pre} $ |
| $MSE = \frac{\sum_{i=1}^n (Y_{exp} - Y_{pre})^2}{n}$ |
| $RMSE = \sqrt{\frac{\sum_{i=1}^n (Y_{exp} - Y_{pre})^2}{n}}$ |
| $AAE = \frac{1}{n} \sum_{i=1}^n \left \frac{Y_{i,exp} - Y_{i,pre}}{Y_{i,exp}} \right $ |

Gradient descent and least squares are used to determine contexts and parameters in hybrid learning. For its predictive purposes, ANFIS currently uses an advanced rapid-learning technique called hybrid learning. It has been established by many scientists that hybrid algorithms are effective [39, 40].

3.4. Response Surface Methodology (RSM). As well as optimizing new systems or processes, RSM is frequently used to optimize existing ones as well [18, 23, 37]. Since RSM uses a partial factorial design, the design of experiments can be improved to perform the minimum number of experiments while reducing costs and time. Model accuracy can be deter-

TABLE 5: Comparison between the simulated result and the reported data.

| Parameters | Unit | Model | Turn et al. [45] | Hu et al. [44] |
|---------------------|---------|--------|------------------|----------------|
| Input | | | | |
| Steam/biomass | Ratio | 2.0 | 1.84 | 1.41 |
| Reactor pressure | Bar | 1.0 | 1.0 | 1.0 |
| Reactor temperature | °C | 850 | 800 | 800 |
| Output | | | | |
| H ₂ | Mol/mol | 0.5862 | 0.513 | 0.4701 |
| Energy | MJ/kg | 138.7 | | |

TABLE 6: ANN prediction model error analysis with different hidden neurons for hydrogen.

| Error analysis indicators | 3 | 4 | 5 |
|---------------------------|--------|--------|--------|
| R ² | 0.9355 | 0.9397 | 0.935 |
| MAE | 0.0153 | 0.0147 | 0.0151 |
| MSE | 0.0006 | 0.0005 | 0.0006 |
| RMSE | 0.0236 | 0.0232 | 0.0237 |
| AAE | 0.0475 | 0.0428 | 0.0422 |

mined by calculating the regression coefficient (R²) and adjusted regression coefficient (R²adj), both of which range from 0 to 1.0. Models with high R² and R²adj values (more than 0.9%) are considered precise [18]. A good model should have a difference between R² and R²adj less than

TABLE 7: ANFIS prediction model error analysis with ANFIS type for hydrogen production.

| Error analysis indicators | ANFIS-grid partitioning (ANFIS-GP) | ANFIS-subtractive clustering (ANFIS-SC) | ANFIS-fuzzy c-means (ANFIS-FCM) |
|---------------------------|---------------------------------------|--|------------------------------------|
| R^2 | 0.9993 | 0.9993 | 0.9977 |
| MAE | 0.0013 | 0.0014 | 0.0023 |
| MSE | 0.0000 | 0.0000 | 0.0000 |
| RMSE | 0.0023 | 0.0025 | 0.0044 |
| AAE | 0.0040 | 0.0041 | 0.0063 |

0.2 for the degree of fit determined by R^2 [41]. Here is the 2nd-order quadratic equation for the response-variable equation [42].

$$p = \partial_0 + \sum_{i=1}^n \partial_i u_i + \sum_{i=1}^n \partial_{ii} u_i^2 + \sum \sum \partial_{ij} u_i u_j. \quad (13)$$

Here, “ p ” represents the response variable; “ u ” represents input variables; “ n ” denotes the number of variables; ∂_0 , ∂_i , ∂_{ii} , and ∂_{ij} indicate constant, linear, square, and interaction terms, respectively.

The following equations define each of the statistical parameters used for model evaluation as mentioned in Table 4 [40, 43].

In this case, R^2 , MAE, MSE, RMSE, and AAE are, respectively, the coefficient of determination, the mean absolute error, the mean square error, the root mean square error, and the average absolute error. Optimal matching of data points occurs when the prediction error approaches zero [1].

4. Results and Discussion

4.1. Model Evaluation for ASPEN plus. Table 5 shows the output and input of the process simulation model used to simulate the gasification of corn cobs. Syngas compositions were predicted using ASPEN Plus software, but certain assumptions were considered, leading to some uncertainty, for instance, an underestimation of CH_4 content. A reliability inspection is therefore required before any further investigations can be conducted. Gasifier models must be validated with different experimental studies to ensure their authenticity and accuracy [44, 45]. As reported in published experimental studies, biomass feeds are validated using the same thermodynamic properties [14].

4.2. Model Evaluation for Predictive Potential. The model capability was evaluated using the following statistical parameters: R^2 , MAE, MSE, RMSE, and AAE which are the coefficient of determination, the mean absolute error, the mean square error, the root mean square error, and the average absolute error, respectively. ASPEN Plus, backpropagation neural networks, and ANFIS models were evaluated to predict hydrogen production. For various models, results are shown in Tables 6, 7, and 8. Figures 4 and 5 represent parity plots between experimental data and predicted values; in addition, Tables 6 and 7 show different trial results of the three models involved in this study. However, R^2

TABLE 8: Summary of the different best models for the prediction of hydrogen production.

| Error analysis indicators | ANN | ANFIS-grid partitioning (GP) |
|---------------------------|--------|------------------------------|
| R^2 | 0.9397 | 0.9993 |
| MAE | 0.0147 | 0.0013 |
| MSE | 0.0005 | 0.0000 |
| RMSE | 0.0232 | 0.0023 |
| AAE | 0.0428 | 0.0040 |

should be close to unity (1) to achieve a strong correlation between experimental and expected values. In all three models, R^2 was close to one, indicating strong compatibility [37]. Furthermore, for each model, the RMSE and MSE square root were calculated. All of the values obtained for MSE and RMSE were low, confirming that all of the models used are within range. AAE and MAE calculate a model’s precision and accuracy as displayed in Tables 6 and 7; however, Table 8 expresses the summary of the best results of the two predictive models for comparison. The model of ANFIS-grid partitioning (GP) was able to predict hydrogen production more closely than the best of BP-ANN with two hidden layers (4-4-5-2), based on statistical index results.

4.3. Relationship of Gasification with Steam-to-Biomass Ratio (S/B). The gasification of biomass is characterized by the following main reactions. The results of steam gasification of corn cob feedstock at 850°C with different steam-to-biomass (S/B) ratios are shown in Figure 6(a). H_2 increased with an increase in S/B from 0.8 to 2.0, while CO and CH_4 content decreased. Gas composition could change with a change in S/B for two reasons. Exothermic water-gas shift reactions occur when steam is added to the gasification system (Eq. (10)), and steam reforming of methane being endothermic methods (Eqs. (6)–(9)) consumed CO and CH_4 , increasing [44] H_2 and CO_2 content while decreasing CO and CH_4 . Le Chatelier’s principle could explain the second reason. By adding steam (reactant) to the gasification system, reactions shift toward products, increasing H_2 production. According to Hu et al. [44], the same trend could be explained by an increase in steam reforming and shifting reactions because of the increased S/B. With an increase in S/B from 0.8 to 2.0, Figure 6(a) shows a slight increase in H_2 content. Steam can limit cracking and endothermic reactions like water-gas (equations (6)–(8)) and Boudouard reactions (equation (9)) caused by the addition of a

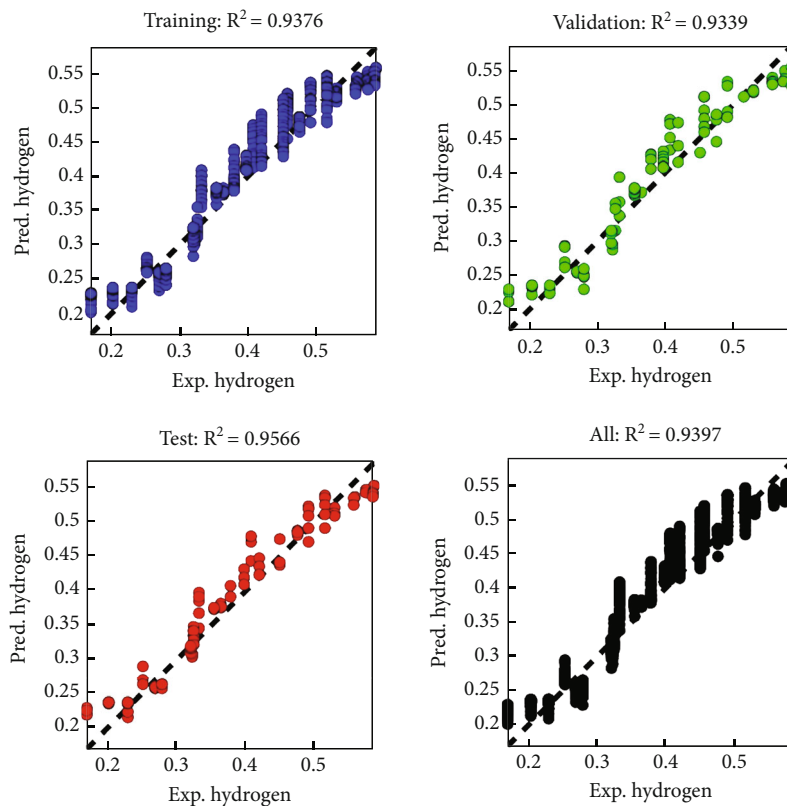


FIGURE 4: The parity plot of experimental hydrogen against predicted hydrogen using the ANN model.

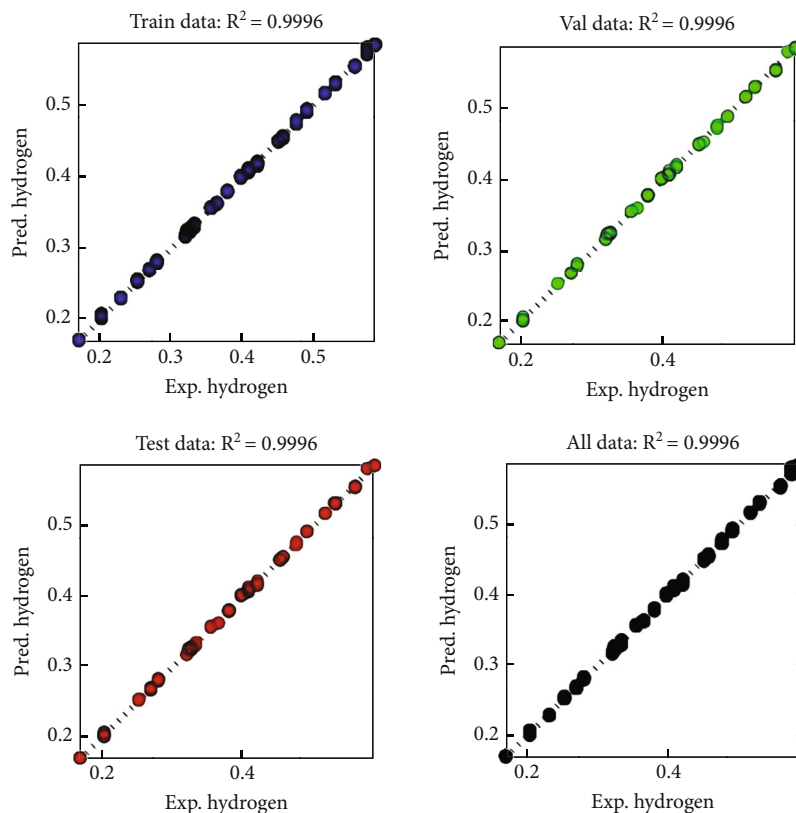


FIGURE 5: Experimental hydrogen against predicted hydrogen using ANFIS model.

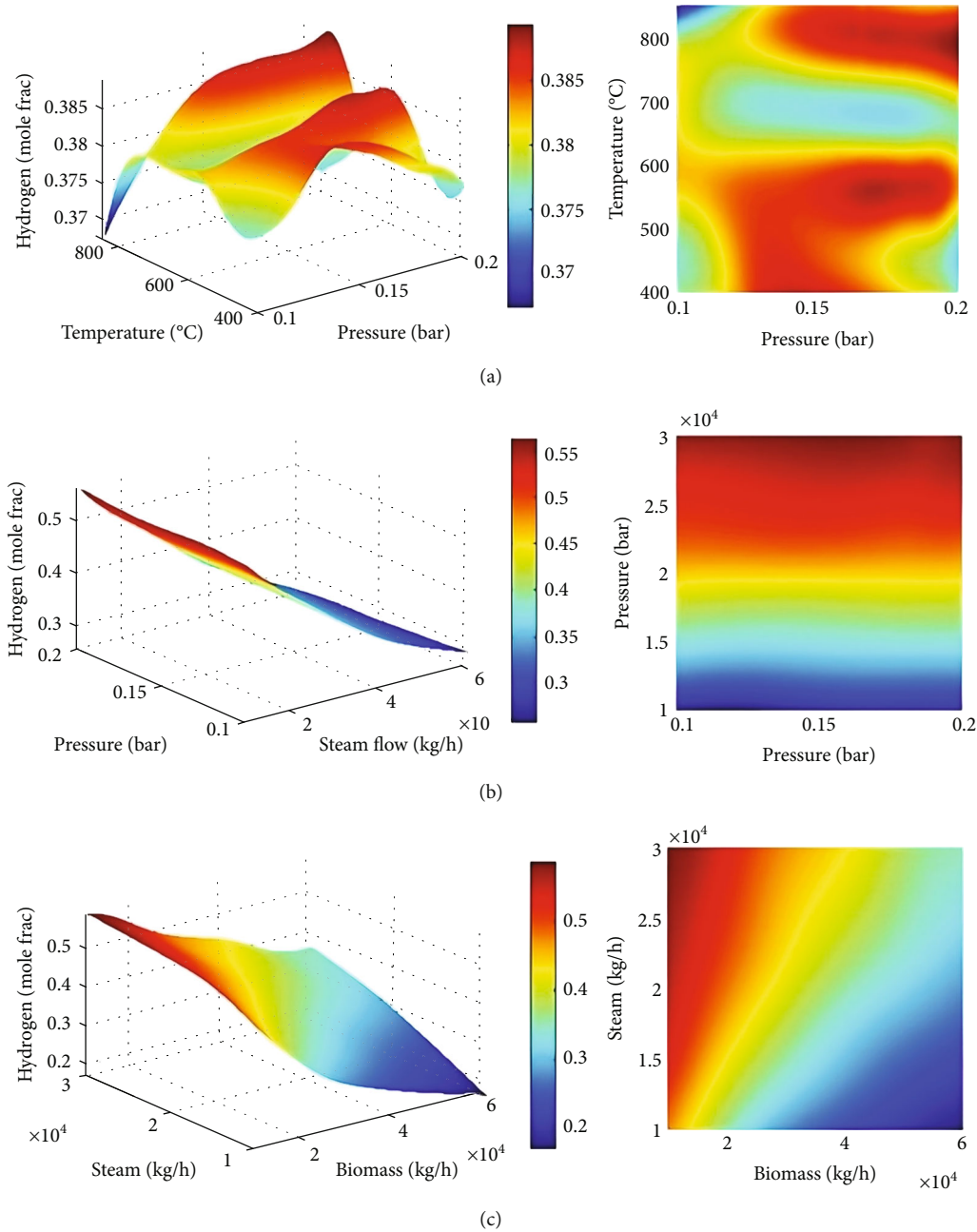


FIGURE 6: (a–c) The 2D and 3D diagrams of the effect of various controlled variables on H_2 .

significant increase in steam quantity. Low S/Bs, however, had less effect since the composition of the gas remained the same. For the production of syngas, it seems reasonable to use higher S/B values (>1.4). While keeping the gasification temperature constant at 850°C , S/B varied from 0.8 to 1.2. It defines the further use of the syngas produced by biomass gasification by measuring H_2/CO . As S/B increased, H_2/CO trended upwards. Gas quality was shown to be affected in two opposite ways by steam addition. A higher S/B results in a higher dry gas yield and char yield [46].

4.4. Gasification Temperature and Gasification Control Variables. Figures 6(b) and 6(c) show the composition of gas at various temperatures with S/B at a constant value.

By steam-gasifying biomass at 650 to 850°C , 22% of CO was produced, while CH_4 and CO_2 contents were decreased. The CO_2 generated by shifting, cracking, and reactions (eqn. (10) and eqns. (6)–(9)) and consumed by the Boudouard reaction were similar to Mazumder and de Lasa [47], however taking these trends into account. Increasing gasification temperature led to an increase in CO_2 consumption rate, which decreased CO concentration. Due to the enhanced endothermic water-gas reaction (eqn. (10)) as the temperature increased, H_2 content increased slightly. Enhanced water-gas reactions (equation (10)) and Boudouard reactions (eqn. (4)) result in a rise in CO content as a result of a rise in gasification temperature. As a result, increasing gasification temperature leads to a greater rate of methane-

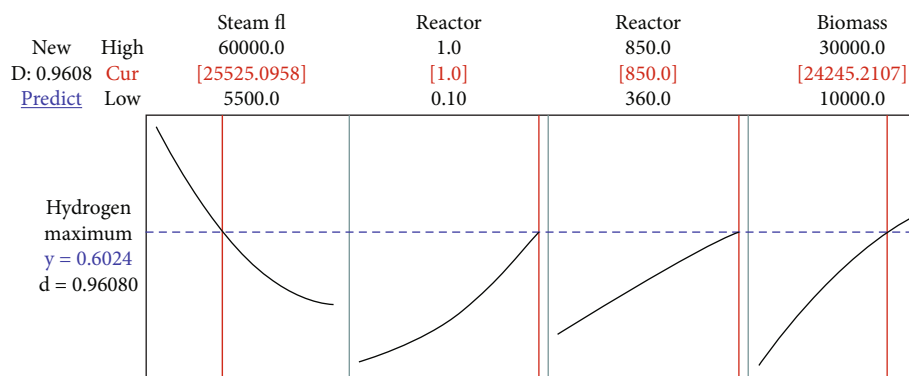


FIGURE 7: Optimization of hydrogen production and energy content from the gasification process.

steam reforming reaction (equation (10)) and decreases the amount of CH_4 . The products in endothermic reactions such as 1 and 2 are favored by Le Chatelier's principle when the temperature is higher.

4.5. Model Optimization and Validation. The maximum hydrogen value obtained using ASPEN Plus for the gasification of the biomass, corn cob with the input parameters such as steam flow of 60000 kg/h, the reactor pressure of 1 bar, the reactor temperature of 850°C, and the biomass flow of 30000 kg/h is 0.5862 mole fraction. Minitab 17 software (RSM) was used to estimate the optimum hydrogen produced from the process simulator in mole fraction, which was 0.6024 as shown in Figure 7. The input parameters were estimated to be a steam flow of 25525.1 kg/h, the reactor pressure was 1 bar, the reactor temperature was 850°C, and the biomass flow was 24245.2 kg/h. While ANFIS was also used to predict the mole fraction of hydrogen produced to be 0.5045, with the input parameters of steam flow, 60000 kg/h, the reactor pressure was 1 bar, the reactor temperature was 848°C, and the biomass flow was 24500 kg/h. The average hydrogen produced of 0.5085 (mole fraction) was obtained using the ASPEN Plus to validate the predicted optimal value with the experimental data. Predictive optimal model value and operational plant value were in good agreement.

5. Conclusion

The feasibility of producing syngas using corn cobs as biomass of choice was evaluated. The study performed a process simulation of steam gasification using the ASPEN Plus simulator. Using experimental data from the literature, the simulated results were validated. In addition to the gasification temperature, the steam-to-biomass ratio results in various effects on gas composition, gas yield, char yield, and H_2/CO . Based on the simulated results, the yield of the gas was positively influenced by an increase in steam-to-biomass ratio from 0.8 to 2.0. The simulations show that an acceptable level of H_2/CO gas could be produced under certain conditions such as steam flow of 23854.6 kg/h, the reactor pressure was 1 bar, the reactor temperature was 847.9°C, and the biomass flow was 23141.8 kg/h. Compared to the combustion of corn cobs (biomass) and without pre-

treatment, steam gasification significantly increased gas yield but decreased char yield. Due to the need to address the energy concerns, research in this direction using artificial intelligence integrated with process simulation will help provide relevant industrial condition that will give appropriate opportunity for understanding and constructing the optimum design for large-scale production of hydrogen.

5.1. Limitations of the Study. By coupling several gasification technologies, it is possible to overcome the limitations of each technology individually. In spite of this, hydrogen production is expected to incur higher operating costs.

5.2. Future Perspectives and Directions of the Study. The biomass gasification and catalytic gasification mechanisms must be determined in order to optimize H_2 yield and control product composition. Moreover, integrating multiple gasification technologies will produce more hydrogen, as well as lower cost of production.

Data Availability

Data is available on reasonable request from the corresponding author.

Conflicts of Interest

The authors declare that they have no conflicts of interest

Authors' Contributions

Conceptualization, review, simulation, supervision, and modeling were conducted by Anthony I. Okoji; cosupervision, analysis, interpretation, review, and editing were conducted by Abiola E. Taiwo; analysis and interpretation were conducted by John Busayo Adeoye; review and editing were conducted by Paul Musonge; writing of the first draft preparation was conducted by David Olamide Makinde; review and editing were conducted by Comfort Nneka Okoji.

Acknowledgments

Open access funding is enabled and organized by SANLiC Gold.

References

- [1] D. R. Nhuchhen and P. A. Salam, "Estimation of higher heating value of biomass from proximate analysis: a new approach," *Fuel*, vol. 99, pp. 55–63, 2012.
- [2] A. Özyüğüran and S. Yaman, "Prediction of calorific value of biomass from proximate analysis," *Energy Procedia*, vol. 107, pp. 130–136, 2017.
- [3] A. E. Taiwo, T. F. Madzimbamuto, and T. V. Ojumu, "Development of an Integrated Process for the Production and Recovery of Some Selected Bioproducts From Lignocellulosic Materials," in *Valorization of Biomass to Value-Added Commodities*, Green Energy and Technology, M. Daramola and A. Ayeni, Eds., Springer, Cham, 2020.
- [4] Y. A. Amran, Y. M. Amran, R. Alyousef, and H. Alabduljabbar, "Renewable and sustainable energy production in Saudi Arabia according to Saudi Vision 2030; current status and future prospects," *Journal of Cleaner Production*, vol. 247, article 119602, 2020.
- [5] E. Betiku and A. E. Taiwo, "Modeling and optimization of bioethanol production from breadfruit starch hydrolyzate vis-à-vis response surface methodology and artificial neural network," *Renewable Energy*, vol. 74, pp. 87–94, 2015.
- [6] M. I. Oloko-Oba, A. E. Taiwo, S. O. Ajala, B. O. Solomon, and E. Betiku, "Performance evaluation of three different-shaped bio-digesters for biogas production and optimization by artificial neural network integrated with genetic algorithm," *Sustainable Energy Technologies and Assessments*, vol. 26, pp. 116–124, 2018.
- [7] C. J. Quarton, O. Tlili, L. Welder et al., "The curious case of the conflicting roles of hydrogen in global energy scenarios," *Sustainable Energy & Fuels*, vol. 4, no. 1, pp. 80–95, 2020.
- [8] T. Rasheed, M. T. Anwar, N. Ahmad et al., "Valorisation and emerging perspective of biomass based waste-to-energy technologies and their socio-environmental impact: a review," *Journal of Environmental Management*, vol. 287, article 112257, 2021.
- [9] C. Park, R. K. Joshi, E. Falascino et al., "Biomass gasification: sub-pilot operation of >600 h with extensive tar cracking property and high purity syngas production at H₂: CO ratio~2 using moving bed redox looping technology," *Fuel Processing Technology*, vol. 252, article 107966, 2023.
- [10] R. Hasanzadeh, T. Azdast, M. Mojaver, and C. B. Park, "High-efficiency and low-pollutant waste polystyrene and waste polystyrene foam gasification: comprehensive comparison analysis, multi-objective optimization and multi-criteria decision analysis," *Fuel*, vol. 316, article 123362, 2022.
- [11] R. Hasanzadeh, P. Mojaver, A. Chitsaz, M. Mojaver, M. Jalili, and M. A. Rosen, "Biomass and low-density polyethylene waste composites gasification: orthogonal array design of Taguchi technique for analysis and optimization," *International Journal of Hydrogen Energy*, vol. 47, no. 67, pp. 28819–28832, 2022.
- [12] G. Li, Y. Chang, L. Chen et al., "Process design and economic assessment of butanol production from lignocellulosic biomass via chemical looping gasification," *Bioresource Technology*, vol. 316, article 123906, 2020.
- [13] X. Zhang, H. Li, L. Liu et al., "Thermodynamic and economic analysis of biomass partial gasification process," *Applied Thermal Engineering*, vol. 129, pp. 410–420, 2018.
- [14] L. P. R. Pala, Q. Wang, G. Kolb, and V. Hessel, "Steam gasification of biomass with subsequent syngas adjustment using shift reaction for syngas production: an Aspen Plus model," *Renewable Energy*, vol. 101, pp. 484–492, 2017.
- [15] A. J. Keche, A. P. R. Gaddale, and R. G. Tated, "Simulation of biomass gasification in downdraft gasifier for different biomass fuels using ASPEN PLUS," *Clean Technologies and Environmental Policy*, vol. 17, no. 2, pp. 465–473, 2015.
- [16] J. H. Pauls, N. Mahinpey, and E. Mostafavi, "Simulation of air-steam gasification of woody biomass in a bubbling fluidized bed using Aspen Plus: a comprehensive model including pyrolysis, hydrodynamics and tar production," *Biomass and Bioenergy*, vol. 95, pp. 157–166, 2016.
- [17] R. Hasanzadeh, P. Mojaver, T. Azdast, S. Khalilarya, and A. Chitsaz, "Developing gasification process of polyethylene waste by utilization of response surface methodology as a machine learning technique and multi-objective optimizer approach," *International Journal of Hydrogen Energy*, vol. 48, no. 15, pp. 5873–5886, 2023.
- [18] P. Mojaver, S. Khalilarya, and A. Chitsaz, "Multi-objective optimization using response surface methodology and exergy analysis of a novel integrated biomass gasification, solid oxide fuel cell and high-temperature sodium heat pipe system," *Applied Thermal Engineering*, vol. 156, pp. 627–639, 2019.
- [19] B. Chalermisinsuwan, Y.-H. Li, and K. Manatura, "Optimization of gasification process parameters for COVID-19 medical masks using response surface methodology," *Alexandria Engineering Journal*, vol. 62, pp. 335–347, 2023.
- [20] P. Mojaver, R. Hasanzadeh, A. Chitsaz, T. Azdast, and M. Mojaver, "Tri-objective central composite design optimization of co-gasification of eucalyptus biomass and polypropylene waste," *Biomass Conversion and Biorefinery*, vol. 14, no. 4, pp. 4829–4841, 2022.
- [21] M. Amiri, A. A. Najafi, and K. Gheshlaghi, "Response surface methodology and genetic algorithm in optimization of cement clinkering process," *Journal of Applied Sciences*, vol. 8, no. 15, pp. 2732–2738, 2008.
- [22] M. Ozonoh, B. Oboirien, and M. Daramola, "Optimization of process variables during torrefaction of coal/biomass/waste tyre blends: application of artificial neural network & response surface methodology," *Biomass and Bioenergy*, vol. 143, article 105808, 2020.
- [23] M. Inayat, S. A. Sulaiman, M. Shahbaz, and B. A. Bhayo, "Application of response surface methodology in catalytic co-gasification of palm wastes for bioenergy conversion using mineral catalysts," *Biomass and Bioenergy*, vol. 132, article 105418, 2020.
- [24] D. Fozer, B. Kiss, L. Lorincz, E. Szekely, P. Mizsey, and A. Nemeth, "Improvement of microalgae biomass productivity and subsequent biogas yield of hydrothermal gasification via optimization of illumination," *Renewable Energy*, vol. 138, pp. 1262–1272, 2019.
- [25] S. Uslu, "Optimization of diesel engine operating parameters fueled with palm oil-diesel blend: comparative evaluation between response surface methodology (RSM) and artificial neural network (ANN)," *Fuel*, vol. 276, p. 117990, 2020.
- [26] M. Wróbel, K. Mudryk, M. Jewiarz, S. Głowacki, and W. Tulej, "Characterization of selected plant species in terms of energetic use. Renewable Energy Sources: Engineering, Technology," in *Innovation: ICORES 2017*, pp. 671–681, Springer, 2018.
- [27] A. Anukam, B. P. Goso, O. O. Okoh, and S. N. Mamphweli, "Studies on characterization of corn cob for application in a

- gasification process for energy production,” *Journal of Chemistry*, vol. 2017, Article ID 6478389, 9 pages, 2017.
- [28] M. Formica, S. Frigo, and R. Gabbrielli, “Development of a new steady state zero-dimensional simulation model for woody biomass gasification in a full scale plant,” *Energy Conversion and Management*, vol. 120, pp. 358–369, 2016.
- [29] S. Rupesh, C. Muraleedharan, and P. Arun, “ASPEN Plus modelling of air–steam gasification of biomass with sorbent enabled CO₂ capture,” *Resource-Efficient Technologies*, vol. 2, no. 2, pp. 94–103, 2016.
- [30] R. Hasanazadeh, P. Mojaver, S. Khalilarya, and T. Azdast, “Air co-gasification process of LDPE/HDPE waste based on thermodynamic modeling: hybrid multi-criteria decision-making techniques with sensitivity analysis,” *International Journal of Hydrogen Energy*, vol. 48, no. 6, pp. 2145–2160, 2023.
- [31] M. A. Adnan and M. M. Hossain, “Gasification performance of various microalgae biomass—a thermodynamic study by considering tar formation using Aspen Plus,” *Energy Conversion and Management*, vol. 165, pp. 783–793, 2018.
- [32] Y. Chen, G. Yu, Y. Long et al., “Application of radial basis function artificial neural network to quantify interfacial energies related to membrane fouling in a membrane bioreactor,” *Bioresource Technology*, vol. 293, article 122103, 2019.
- [33] M. Shahbaz, S. Yusup, A. Inayat, D. O. Patrick, A. Pratama, and M. Ammar, “Optimization of hydrogen and syngas production from PKS gasification by using coal bottom ash,” *Bioresource Technology*, vol. 241, pp. 284–295, 2017.
- [34] D. Wu, D. Zhang, S. Liu et al., “Prediction of polycarbonate degradation in natural atmospheric environment of China based on BP-ANN model with screened environmental factors,” *Chemical Engineering Journal*, vol. 399, article 125878, 2020.
- [35] X. Zhang, S.-Y. Lee, H. Luo, and H. Liu, “A prediction model of sleep disturbances among female nurses by using the BP-ANN,” *Journal of Nursing Management*, vol. 27, no. 6, pp. 1123–1130, 2019.
- [36] H. Demuth and M. Beale, *Neural Network Toolbox for Use with MATLAB: User's Guide; Computation, Visualization, Programming*, MathWorks Incorporated, 2000.
- [37] A. Okoji, A. Anozie, and J. Omoleye, “Evaluation of optimization techniques for predicting exergy efficiency of the cement raw meal production process,” *Cogent Engineering*, vol. 8, no. 1, article 1930493, 2021.
- [38] A. I. Okoji, A. N. Anozie, J. A. Omoleye, A. E. Taiwo, and D. E. Babatunde, “Evaluation of adaptive neuro-fuzzy inference system-genetic algorithm in the prediction and optimization of NO_x emission in cement precalcining kiln,” *Environmental Science and Pollution Research*, vol. 30, no. 19, pp. 54835–54845, 2023.
- [39] C. Okoji, A. I. Okoji, M. S. Ibrahim, and O. Obinna, “Comparative analysis of adaptive neuro-fuzzy inference system (ANFIS) and RSRM models to predict DBP (trihalomethanes) levels in the water treatment plant,” *Arabian Journal of Chemistry*, vol. 15, no. 6, article 103794, 2022.
- [40] N. VU-Bac, T. Lahmer, Y. Zhang, X. Zhuang, and T. Rabczuk, “Stochastic predictions of interfacial characteristic of polymeric nanocomposites (PNCs),” *Composites Part B: Engineering*, vol. 59, pp. 80–95, 2014.
- [41] Ö. Çelebican, İ. İnci, and N. Baylan, “Modeling and optimization of formic acid adsorption by multiwall carbon nanotube using response surface methodology,” *Journal of Molecular Structure*, vol. 1203, article 127312, 2020.
- [42] T. Detchusananard, K. Im-Orb, F. Maréchal, and A. Arpornwihanop, “Analysis of the sorption-enhanced chemical looping biomass gasification process: performance assessment and optimization through design of experiment approach,” *Energy*, vol. 207, article 118190, 2020.
- [43] M. Jian, Z. Hongdong, and Y. Jingjing, “Development and application of artificial neural networks,” *Electronic Design Engineering*, vol. 24, 2011.
- [44] Y. Hu, Q. Cheng, Y. Wang et al., “Investigation of biomass gasification potential in syngas production: characteristics of dried biomass gasification using steam as the gasification agent,” *Energy & Fuels*, vol. 34, pp. 1033–1040, 2019.
- [45] S. Turn, C. Kinoshita, Z. Zhang, D. Ishimura, and J. Zhou, “An experimental investigation of hydrogen production from biomass gasification,” *Hydrogen Energy*, vol. 23, no. 8, pp. 641–648, 1998.
- [46] F. Kartal and U. Özveren, “A comparative study for biomass gasification in bubbling bed gasifier using Aspen HYSYS,” *Bioresource Technology Reports*, vol. 13, article 100615, 2021.
- [47] J. Mazumder and H. I. De Lasa, “Catalytic steam gasification of biomass surrogates: thermodynamics and effect of operating conditions,” *Chemical Engineering Journal*, vol. 293, pp. 232–242, 2016.